Release of IFN-γ by acute myeloid leukemia cells remodels bone marrow immune microenvironment by inducing regulatory T cells

Giulia Corradi,[1#] Barbara Bassani,[2#] Giorgia Simonetti,[3] Sabina Sangaletti,[2] Jayakumar Vadakekolathu,[4] Maria Chiara Fontana,[3] Martina Pazzaglia,[3] Alessandro Gulino,[5] Claudio Tripodo,[5] Gianluca Cristiano,[1] Lorenza Bandini,[6] Emanuela Ottaviani,[6] Giovanni Martinelli,[3] Mario Paolo Colombo,[2] Sergio Rutella,[4,7] Michele Cavo,[1,6] Marilena Ciciarello*[8] and Antonio Curti*[6]

[1] Dipartimento di Medicina Specialistica, Diagnostica e Sperimentale, Università di Bologna, Bologna, Italy; [2] Fondazione IRCCS, Istituto Nazionale dei Tumori, Milan, Italy; [3] IRCCS Istituto Romagnolo per lo Studio dei Tumori "Dino Amadori"-IRST, Meldola (FC), Italy; [4] John van Geest Cancer Research Centre, College of Science and Technology, Nottingham Trent University, Nottingham, UK; [5] Tumor Immunology Unit, Department of Health Sciences, University of Palermo, Palermo, Italy; [6] IRCCS Azienda Ospedaliero-Universitaria di Bologna, Istituto di Ematologia "Seràgnoli", Bologna, Italy; [7] Centre for Health, Ageing and Understanding Disease (CHAUD), Nottingham Trent University Clifton Campus, Nottingham, UK. [8] Istituto di Ematologia "Seràgnoli", Bologna, Italy

[#] G.C. and B.B. contributed equally to this study.

* M. Ciciarello and A.C. contributed equally to this study.

Running title: IFN-γ and leukemic microenvironment

Keywords: IFN-γ, acute myeloid leukemia, leukemic microenvironment, regulatory T cells, stromal microenvironment

Financial support: this research was supported by FATRO/Foundation Corrado and Bruno Maria Zaini-Bologna, Fabbri1905 and Bologna AIL (Associazione Italiana contro le Leucemie)/Section of Bologna, Associazione Italiana per la Ricerca sul Cancro (IG22204 to SS and IG20654 to AC). MC was supported by the University of Bologna (Alma Idea Junior Grant 2017) and the American Society of Hematology (ASH)/Giuseppe Bigi Memorial Award. BB is funded by the FIRC-AIRC

(Fondazione Italiana per la Ricerca sul Cancro) fellowship "Guglielmina Lucatello e Gino Mazzega".

Correspondence: Prof. Michele Cavo, Istituto di Ematologia "Seràgnoli", Dipartimento di Medicina Specialistica, Diagnostica e Sperimentale, Università di Bologna
Via Massarenti 9, 40138 Bologna, Italy. Tel: +39-0512143809, +39-0512143537; Fax: +39-051398973; e-mail: michele.cavo@unibo.it

Marilena Ciciarello, Ph.D., Istituto di Ematologia "Seràgnoli", Dipartimento di Medicina Specialistica, Diagnostica e Sperimentale, Università di Bologna, Via Massarenti 9, 40138 Bologna, Italy. Tel.: +39-0512143064; Fax: +39-0512144037; e-mail: marilena.ciciarello2@unibo.it

Authors' Disclosures

The authors declare no potential conflicts of interest.

Word count: 4292

Number of figures and tables: 6

Translational significance

In most tumors, IFN-γ provides a signal resulting in enhanced anti-tumor immunity and better clinical outcome. By contrast, our study reveals the "dark side" of IFN-γ in the creation of an immune-tolerant microenvironment enriched in Tregs and correlated with a worse prognosis in AML patients. *In vitro* and *in vivo* results demonstrate that IFN-γ released by AML cells, not by leukemia-infiltrating immune cells, remodels the BM immune and stromal microenvironment by inducing suppressive Tregs. Given the emerging role of immunotherapies for AML, our findings support the incorporation of a new panel of microenvironment-based immunological factors into current AML classification and prognostication systems. Moreover, a greater understanding of the IFN-γ-dependent tolerogenic tuning of the BM microenvironment provides the rationale for therapies targeting IFN-γ-driven immune-modulatory effects on stromal and immune AML microenvironment, i.e., IDO1 inhibitors, and combining the activation of effector cells with the inhibition of Tregs.

Abstract

Purpose: The stromal and immune bone marrow (BM) landscape is emerging as a crucial determinant for acute myeloid leukemia (AML). Regulatory T cells (Tregs) are enriched in the AML microenvironment, but the underlying mechanisms are poorly elucidated. Here, we addressed the effect of IFN-γ released by AML cells in BM Tregs induction and its impact on AML prognosis.

Experimental design: BM aspirates from AML patients were subdivided according to *IFNG* expression. Gene expression profiles in *INFG*^{high} and *IFNG*^{low} samples were compared by microarray and NanoString analysis and used to compute a prognostic index. The IFN-γ release effect on the BM microenvironment was investigated in mesenchymal stromal cell (MSC)/AML cell co-cultures. In mice, AML cells silenced for IFN-γ expression were injected intrabone.

Results: *IFNG*^{high} AML samples showed an upregulation of inflammatory genes, usually correlated with a good prognosis in cancer. By contrast, in AML patients, high *IFNG* expression associated with

poor overall survival. Notably, IFN-γ release by AML cells positively correlated with a higher frequency of BM suppressive Tregs. In co-culture experiments, $IFNG^{high}$ AML cells modified MSC transcriptome by up-regulating IFN-γ-dependent genes related to Treg induction, including indoleamine 2,3-dioxygenase 1 (IDO1). IDO1 inhibitor abrogated the effect of IFN-γ release by AML cells on MSC-derived Treg induction. *In vivo*, the genetic ablation of IFN-γ production by AML cells reduced MSC IDO1 expression and Treg infiltration, hindering AML engraftment.

Conclusions: IFN-γ release by AML cells induces an immune-regulatory program in MSCs and remodels BM immunological landscape toward Treg induction, contributing to an immunotolerant microenvironment.

Introduction

Acute myeloid leukemia (AML) is a heterogeneous clonal disease that develops from a rare population of bone marrow leukemic stem cells (1). For many years, cytogenetic and molecular aberrations in hematopoietic stem cells were considered the only causative factors in AML onset and development. Recently, this notion has been challenged, and it is now established that AML pathophysiology also depends on the bone marrow (BM) microenvironment (2,3).

A component of the BM microenvironment that is crucial to AML pathophysiology is the immunological landscape (4,5). Aberrant cytokine production and a profound dysregulation of the frequency and function of immune cell subsets induce an immunosuppressive milieu, which favors the escape of AML cells from immune control (6,7). In particular, the BM microenvironment in AML is enriched in regulatory T cells (Tregs) (8,9), which contribute to the immunosuppressive phenotype (10), chemoresistance, and disease relapse (8,11). The induction and the suppressive functions of Tregs are regulated, among others, by mesenchymal stromal cells (MSCs) (12), recognized as pivotal contributors to the hematopoietic stem cell niche (13). A crucial mediator of MSC-driven Treg induction is indoleamine 2,3-dioxygenase 1 (*IDO1*) (14,15), a well-known tryptophan metabolizing enzyme contributing to the immunosuppressive tumor microenvironment (16). Notably, MSCs are not constitutively immunosuppressive but rather acquire this capacity, including the ability to induce Tregs, in response to pro-inflammatory stimuli (14,15).

Inflammation has recently emerged as a hallmark of cancer (17). Along with its pro-tumorigenic effects, inflammatory signals also influence the host immune response inhibiting tumor development (18). One such signal is interferon (IFN)-γ, a cytokine produced predominantly by T cells and natural killer (NK) cells that suppresses hematopoiesis and is a master regulator of innate and adaptive immunity (19,20). In the tumor microenvironment, IFN-γ orchestrates an array of anti-proliferative, pro-apoptotic, anti-tumor, immune-activating responses (21). IFN-related gene signature is a favorable predictive marker for chemotherapy and radiotherapy efficiency as well as

immunotherapy in various types of malignancies (22,23). However, emerging and seemingly paradoxical findings indicate that IFN-γ can also be involved in pathways supporting tumorigenesis and immune evasion (24).

This study aimed to address whether IFN-γ regulates immunological changes of the BM microenvironment in AML. For this purpose, we used BM aspirates from AML patients, cell-culture systems, and a murine AML model to investigate the ability of AML cells to favor the establishment of a Treg-centered immunosuppressive microenvironment through the release of IFN-γ.

Materials and Methods

The Supplementary Methods detail procedures for primary cell isolation, qRT-PCR, flow cytometry, western blotting, immunohistochemistry, immunofluorescence, and prognostic index calculation.

Ethics statement

This study is part of ongoing research approved by the Independent Ethics Committee of the Area Vasta Emilia Centro (94/2016/O/Tess). AML patients and healthy BM donors were recruited at Seràgnoli Hematology Institute in Bologna. Clinical samples and data were collected with written informed consent. The investigations were conducted in accordance with the Declaration of Helsinki.

Biological samples and cell cultures

BM aspirate samples were collected from 49 AML patients at diagnosis (blasts ≥80%) and 8 healthy donors (Supplementary Table S1). BM samples were used to isolate mononuclear cells. Throughout the text, we referred to IFN-γ^{high} or IFN-γ^{low} AML cells as BM cells in the large majority (≥80%) expressing blast cell-associated markers and co-expressing IFN-γ, respectively above or below the median within our AML patients' cohort. BM samples were also used to isolate MSCs (Supplementary Methods).

GeneChip gene expression profiling

The first part of the study used gene expression data generated for our previous studies, specifically from BM mononuclear cells of 61 AML patients (blasts ≥80%) (GSE161532) (25) and 7 healthy BM donors (not previously reported). The patients include 29 men and 32 women of mean age 60.1 (SD = 11.9) years. In all cases, mononuclear cells had been isolated from BM aspirates by density gradient centrifugation and lysed in RLT buffer (Qiagen). RNA was extracted and reverse-transcribed into cDNA as previously reported (26). cDNA was hybridized to GeneChip Human

Transcriptome Assay 2.0 microarrays (Thermo Fisher Scientific). Data were analyzed using Transcriptome Analysis Console 4.0 software (Thermo Fisher Scientific) and the SST-RMA (signal space transformation – robust multiple-array average) algorithm.

GeneChip data for *IFNG* mRNA were used to dichotomize the AML cell preparations into an $IFNG^{low}$ group (below the median) and $IFNG^{high}$ group (above the median). Then, for all genes, fold change (FC) in expression was calculated as $IFNG^{high}/IFNG^{low}$. Genes with $|FC| \geq 2.0$ and $P \leq 0.05$ (according to Transcriptome Analysis Console software) were considered differentially expressed. A heatmap of differentially expressed genes (DEGs) was generated using ClustVis (27). DEGs were attributed to macro-pathways according to pathway analysis and functional annotation (GeneCards) and analyzed using Enrichr (https://amp.pharm.mssm.edu/Enrichr/)(28).

Amplification-free gene expression profiling

Messenger RNA was extracted from BM mononuclear cells of AML patients (18 men and 6 women; mean age, 53.4 years; SD=17.6 years) (Supplementary Table S1) using Maxwell RSC simplyRNA Blood Kit (Promega). Samples (100-150 ng) were analyzed on the nCounter FLEX system using the PanCancer IO 360 Panel (NanoString Technologies). Reporter probe counts were analyzed using nSolver software (v4.0.62) and nSolver Advanced Analysis module (v2.0.115). Captured transcript counts were normalized to the geometric mean of the included reference genes and internal positive controls. DEGs between $IFNG^{high}$ and $IFNG^{low}$ groups (based on qRT-PCR) were identified using $|\log2\ FC|>2.0$ and $P<0.05$ (Benjamini–Yekutieli false discovery rate, Student's *t* test). The nSolver software package was used to calculate, for each sample, biological activity, and pathway scores, as linear combinations of pre-defined gene sets. STRING (https://string-db.org/) was used to analyze functional interaction networks.

Co-culture experiments

To study the effects of AML cells on BM-derived MSCs, we used two-chamber co-cultures with MSCs in the lower and AML cells in the upper chamber. Cells were cultured for up to 4 days and recovered for analyses (Supplementary Methods).

Murine model of AML

Animal studies were approved by the Committee for Animal Welfare of Fondazione IRCCS Istituto Nazionale dei Tumori and Italian Ministry of Health (authorization 781/2018-PR) and performed following Italian law D.lgs 26/2014. To create a murine model of AML, the murine acute leukemia cell line C1498 was infected with lentiviral particles containing a vector expressing *Ifng*-specific interfering shRNA (shIFN-γ) or non-specific shRNA (control cells). These cells were injected into the tibias of C57BL/6 mice. BM cells were later obtained for analysis (Supplementary Methods).

Data availability

For the original gene expression data, please contact: giorgia.simonetti@irst.emr.it. For the original NanoString nCounter FLEX data, please contact: sergio.rutella@ntu.ac.uk. Gene expression and Nanostring data have been deposited in NCBI's Gene Expression Omnibus and are accessible through GEO Series accession numbers GSE161532 (AML)(25), GSE155441 (MSCs vs. AML/MSCs), and GSE146204 (NanoString).

Statistical analysis

Tests used in statistical analyses are indicated in the figure legends. $P<0.05$ was considered significant. Analyses were done using GraphPad Prism software (v6.0).

Results

IFNG^{high} AML samples have a gene signature enriched in IFN-γ signaling, inflammatory, and immune-response pathways, which correlates with poor clinical outcome

To clarify the role of IFN-γ signaling in AML, we first compared *IFNG* mRNA levels in BM aspirates of AML patients and healthy donors (**Fig. 1A**). From existing GeneChip microarray data, it emerged that *IFNG* mRNA levels in AML samples had a broad distribution skewed to higher values. The median was used to dichotomize AML samples into IFNG^{low} and IFNG^{high} groups (**Fig. 1B**). Expression levels in IFNG^{low} and IFNG^{high} groups were lower and higher, respectively, than in samples from healthy BM donors.

To determine whether the groups of AML cells differed in overall gene expression, we used the same data to identify differentially expressed genes (DEGs) and found 47 up-regulated and 19 down-regulated genes in the IFNG^{high} group compared to the IFNG^{low} group (**Fig. 1C,** DataSheet_page1). Ranking DEGs in macro-pathways revealed that 19 genes belonged to inflammation and immune response pathways. Notably, the IFNG^{high} group had lower expression levels of genes involved in immune responses (e.g., *CIITA*, *CD180*, *CD1C*) and higher expression levels of genes involved in inflammation (e.g., *CXCL8*, *CCL4, CXCL2*). Enrichment analysis revealed that the DEGs were involved in IFN-γ response pathways, including cytokine-mediated signaling, among other pathways (Supplementary Table S2).

To further investigate this phenomenon, we analyzed 24 BM samples of AML patients. qRT-PCR on *IFNG* mRNA was used to dichotomize samples into IFNG^{high} and IFNG^{low} groups. The expression of 750 cancer-related genes was profiled in an amplification-free manner on the nCounter platform using the PanCancer IO 360 Panel (NanoString). Samples classified as IFNG^{high} expressed significantly higher levels of *IFNG* mRNA than IFNG^{low} AML samples (Supplementary Fig. S1A).

These data were then used to identify DEGs between IFNG^{high} and IFNG^{low} groups (**Fig. 2A**, DataSheet_page2). *CD28*, *CXCL8 GZMH*, *GZMA*, *IFIT1, CD8A*, and *CD3G* were among the most significantly up-regulated genes in IFNG^{high} samples, corroborating the relationship between high *IFNG* expression and modulated IFN-γ signaling observed above (**Fig. 1C;** Supplementary Table S2). Pathway analysis revealed an enrichment of DEGs in KEGG pathways related to T cell receptor signaling, Th1 and Th2 cell differentiation, Wnt, and NF-κB signaling (Supplementary Table S3). Network interaction analysis showed the DEGs involved in molecular pathways known to be enriched in solid cancers (Supplementary Fig. S1B).

We then used the DEGs to compute 25 biological activity and pathway scores (**Fig. 2B**). IFNG^{high} samples expressed higher levels of genes belonging to PI3K-Akt, MAPK, JAK/STAT, and NF-κB signaling pathways. In contrast, IFNG^{low} samples had increased expression of gene sets reflecting epigenetic regulation, DNA damage repair, cellular proliferation, and autophagy.

Finally, using NanoString data for all 24 samples, we examined correlations in expression between *IFNG* and genes activated by IFN-γ signaling (**Fig. 2C**). *IFNG* expression correlated positively with that of *IDO1*, nitric oxide synthase 2 (*NOS2*), interferon regulatory factor 1 (*IRF1*), and granzymes *GZMB* and *GZMM*, but not programmed death-ligand 1 (*PD-L1*).

These results prompted us to evaluate the impact of *IFNG* expression on the clinical outcomes of AML patients. We computed a prognostic index (PI), as previously published (29), based on expression levels of the 30 DEGs from our NanoString analysis (DataSheet_page2), which was applied to 149 cases of non-promyelocytic AML from the TGCA project (30). Survival analysis revealed that patients whose PI was above the median had significantly shorter overall survival than those with a PI below the median (**Fig. 2D**). Remarkably, only the up-regulated genes contributed to poor survival; the down-regulated genes were not prognostic (Supplementary Fig. S1C and S1D).

Overall, these data suggest that IFNG^{high} and IFNG^{low} AML samples express distinct gene signatures. Intriguingly, along with genes belonging to inflammatory pathways, high *IFNG* expression also correlated with high expression of immunosuppressive genes induced by IFN-γ signaling and associated with a poor clinical outcome.

High IFN-γ production by AML cells results in increased Tregs in the BM

We next investigated whether all BM cells synthesize IFN-γ or if specific cell populations were responsible. BM mononuclear cells of AML patients (Supplementary Table S1) were stained for CD3, blast cell-associated markers (i.e., CD34, CD33, or CD117), and intracellular IFN-γ. Flow cytometry showed that a substantial fraction of CD3^{-} cells expressing a blast-surface marker contained IFN-γ (**Fig. 3A**). Similar to *IFNG* mRNA data (**Fig. 1A**), there was high inter-patient variability in the fraction of IFN-γ^{+} AML cells (median, 21.1%; range, 2.1%-67.0%), allowing us to dichotomize at the median into IFN-γ^{high} and IFN-γ^{low} groups (**Fig. 3B,** Supplementary S2A, S2B, and S2C). The mean percentages of IFN-γ^{+} cells in the IFN-γ^{high} and IFN-γ^{low} groups were 35.9% and 6.4%, respectively (**Fig. 3B**). This percentage in the IFN-γ^{high} group was significantly different from that in CD34^{+} cells from healthy BM donors. Similar results were obtained by analyzing the IFN-γ mean fluorescence intensity (Supplementary Fig. S2B). AML samples classified as IFN-γ^{high} and IFN-γ^{low} had similar, low percentages of CD3^{+}, CD8^{+}, NK, and other cell types (**Fig. 3C**). Within these cell populations, the fraction of IFN-γ^{+} cells associated with group assignment (IFN-γ^{high} vs. IFN-γ^{low}) only for AML cells (**Fig. 3D**).

We further investigated the immune cell composition of AML samples according to IFN-γ production by AML cells, and we found that the percentage of CD4^{+}CD25^{+}CD127$^{low/-}$ cells (namely Tregs) (31) was significantly higher in IFN-γ^{high} than in IFN-γ^{low} and healthy donor samples (**Fig. 3E**). Furthermore, there was a positive correlation between the percentages of Tregs and IFN-γ^{+} AML cells (**Fig. 3F**). Notably, the percentage of activated Tregs, which mostly retain suppressive activity among Treg subsets (32) and cytotoxic T-lymphocyte antigen (CTLA)-4^{+}PD-1^{+} suppressive Tregs were

289 higher in IFN-γ^{high} than IFN-γ^{low} samples (**Fig. 3G,** Supplementary Fig. 2D). Consequently, the ratios
290 between Tregs and both $CD4^+$ and $CD8^+$ T effector cells were higher in IFN-γ^{high} than IFN-γ^{low}
291 samples (Supplementary Fig. S2E).

292 These data indicate that, among cells from patients' BM aspirates, AML cells are the main source of
293 IFN-γ. IFN-γ^{high} BM samples do not differ in the percentage of the central immune cells (i.e., $CD3^+$,
294 $CD8^+$, NK cells) compared with IFN-γ^{low} BM samples but are enriched in suppressive Tregs.

295 **IFN-γ^{high} AML cells up-regulate IFN-γ-related immunosuppressive genes in MSCs**
296 MSCs are crucial components of the normal and leukemic BM microenvironment and respond to
297 pro-inflammatory stimuli, especially IFN-γ, by modifying the immunological landscape (14,15).
298 With that in mind, we set up an *in vitro* model to investigate interactions between AML cells (IFN-
299 γ^{high} and IFN-γ^{low}) and AML patient-derived MSCs. For this purpose, two-chamber co-cultures were
300 used. After 4 days of co-culture, IFN-γ^{high} cells maintained significantly higher levels of *IFNG*
301 expression and IFN-γ production than IFN-γ^{low} cells (Supplementary Fig. S3A and S3B), while
302 MSCs did not produce IFN-γ (Supplementary Fig. S3C and S3D). Moreover, there was a
303 significantly higher concentration of IFN-γ in the conditioned medium from co-cultures with IFN-
304 γ^{high} than IFN-γ^{low} cells (**Fig. 4A**).

305 We used a similar model to determine if IFN-γ^{high} and IFN-γ^{low} cells have different effects on MSC
306 gene expression. After 24 h of co-culture, compared to MSC monocultures, we detected 82 up-
307 regulated and 12 down-regulated genes in co-cultures involving IFN-γ^{high} cells, and 17 and 10
308 genes, respectively, in co-cultures with IFN-γ^{low} cells; 14 genes were up-regulated by both
309 conditions (**Fig. 4B**, DataSheet_page3). Interactions with IFN-γ^{high} cells resulted not only in a
310 greater number of altered genes than with IFN-γ^{low} cells but also a different pattern of gene
311 induction or down-regulation (**Fig. 4C**). Interestingly, MSCs co-cultured with IFN-γ^{high} cells had
312 increased expression of genes encoding chemokines (e.g., *CXCL1, CCL5*) implicated in Treg

recruitment in solid tumors (33,34) and of *NFKB2* and *RELB* genes that encode key regulators of *IDO1* (35,36). Importantly, IFN-γ^{high} but not IFN-γ^{low} cells induced MSCs to up-regulate gene sets related to Treg differentiation (**Fig. 4D**). Finally, a set of IFN-γ–dependent immune-modulating pathways, including NF-κB, chemokine, and cytokine signaling, was up-regulated in MSCs co-cultured with IFN-γ^{high} cells (Supplementary Table S4). Taken together, these data suggest that IFN-γ synthesis and secretion by AML cells skews MSC phenotype towards immunosuppression.

IFN-γ release by AML cells *in vitro* drives MSCs to induce Tregs via IDO1

Tregs, the most prominent and fundamental cell population in the BM microenvironment of AML patients (5,7-9), significantly contribute to creating an immune-suppressive phenotype (10). We found that the percentage of Tregs was significantly higher in IFN-γ^{high} than IFN-γ^{low} samples (**Fig. 3E**). Based on the results on MSC transcriptome modifications after cultures with IFN-γ^{high} cells (**Fig. 4C and D**), we asked whether the release of IFN-γ by AML cells induced MSCs to promote Tregs. To this end, we focused on IDO1, widely recognized as the nodal mediator of the IFN-γ-regulated MSC immunomodulatory properties (14). *IDO1* and *IFNG* gene expression were positively correlated in AML samples (**Fig. 2C**), and, among different cytokines, IFN-γ was the most potent stimulus for IDO1 induction in MSCs (Supplementary Fig. S4A and S4B).

Thus, we evaluated *IDO1* expression in MSCs co-cultured for 4 days with IFN-γ^{high} or IFN-γ^{low} AML cells, distinguished as described above (**Fig. 3A**). We found *IDO1* higher expression only with IFN-γ^{high} cells, at both mRNA (**Fig. 5A**) and protein levels (**Fig. 5B**, Supplementary Fig. S4C). An IFN-γ–neutralizing antibody in co-cultures with IFN-γ^{high} cells significantly reduced *IDO1* induction in MSCs (**Fig. 5C**). Similar results were obtained with an anti-IFN-γ receptor antibody (data not shown).

Next, we asked if IDO1 up-regulation by IFN-γ^{high} cells may drive MSCs to induce Tregs. First, we co-cultured IFN-γ^{high} cells and MSCs and then replaced the IFN-γ^{high} cells with PBMCs: flow

cytometry after 7 days showed a significantly higher fraction of $CD3^+CD4^+CD25^+FOXP3^+$ cells (*bona fide* Tregs) in the PBMCs cultured with IFN-γ^{high} cell-conditioned MSCs than in PBMCs cultured alone (**Fig. 5D**). The addition of an IDO1 inhibitor virtually abrogated Treg induction (**Fig. 5D**). We used a Treg conversion assay to measure the induction of $CD4^+CD25^+FOXP3^+$ cells (Tregs) from $CD4^+CD25^-$ cells cultured with IFN-γ^{high} cell-conditioned MSCs. The fraction of Tregs was low in immunomagnetically purified $CD4^+CD25^-$ cells cultured alone but increased significantly when these cells were co-cultured with MSCs previously co-cultured with IFN-γ^{high} cells (**Fig. 5E**, Supplementary Fig. S5A). The inclusion of an IDO1 inhibitor substantially reduced the conversion (**Fig. 5E**, Supplementary Fig. S5A). Interestingly, IFN-γ^{high} AML cells alone were unable to induce $CD4^+CD25^+FOXP3^+$ cells. Finally, in a Treg proliferation assay, similar proliferation indexes were obtained after 7 days of culture with MSCs preconditioned by IFN-γ^{high} cells in comparison with PBMCs alone, indicating that the Treg increase induced by IFN-γ^{high} cell-conditioned MSCs is not due to Treg proliferation (Supplementary Fig. S5B). Altogether, these data suggest that IFN-γ secretion by AML cells drives MSCs to induce Treg conversion in an IDO1-dependent manner.

IFN-γ secretion by AML cells *in vivo* remodels the BM microenvironment by inducing Tregs and favors leukemia cell engraftment

To gain insight into the effects of AML cell-derived IFN-γ on the BM microenvironment, we established a murine model of AML. For this purpose, we chose the C1498 murine leukemia cell line, which expresses the *Ifng* gene (Supplementary Fig. S6A), and we used shRNA interference to knock down this gene's expression (Supplementary Fig. S6B). Cells transfected with non-specific or *Ifng*-specific shRNA vectors (control or shIFN-γ cells, respectively) were injected into C57BL/6 mice tibia. Injection of IFN-γ–producing control cells resulted in a diffuse interstitial effacement of BM parenchyma (Supplementary Fig. S6C) that was coherent with localization of AML cells (as previously described (37)). After 31 days, mice were sacrificed, and tibiae were flushed to recover

362 BM cells: flow cytometry showed a significantly higher percentage of engraftment in mice that
363 received control than shIFN-γ cells (**Fig. 6A**).

364 Since *Ifng* knockdown did not modify the intrinsic ability of C1498 cells to proliferate
365 (Supplementary Fig. S6D), we asked whether IFN-γ stimulates leukemic cell engraftment by
366 modifying the BM microenvironment. Flow cytometry of BM cells revealed similar percentages of
367 $CD4^+$ and $CD8^+$ cells (data not shown) but a significantly higher frequency of Tregs in the BM of
368 mice injected with control than shIFN-γ cells (**Fig. 6B**). This Treg expansion was paralleled by a
369 significant increase in a population of Tregs expressing OX40, a Treg-associated fitness marker
370 (Supplementary Fig. S6E). These data suggest that, in AML, high levels of IFN-γ within the BM
371 microenvironment increase Tregs and leukemic cell engraftment.

372 Given these results, we investigated whether the *in vivo* reshaping of the BM microenvironment
373 toward Tregs by IFN-γ–producing AML cells was due to increased IDO1. Immunohistochemistry
374 on BM sections revealed that IDO1 expression was significantly lower in mice injected with shIFN-
375 γ cells than in control (**Fig. 6C** and **D**). Immunofluorescence revealed that IDO1 expression
376 decreased also in MSCs, identified as α–smooth muscle actin $(SMA)^+$/ $nestin^+$ cells (**Fig. 6E**). A
377 similar pattern was obtained for NOS2 (Supplementary Fig. S6F), a downstream target of IFN-γ
378 with a critical role in MSC-mediated immunosuppression (38). Finally, we examined the impact of
379 IFN-γ–producing cells on the population of Tregs expressing CTLA-4, a potent suppressor of cells
380 in the tumor microenvironment (39). The fraction of all Tregs expressing CTLA-4 was higher in
381 BM of mice that received control than shIFN-γ cells, and administration of the IDO1 inhibitor
382 NLG919 to mice inoculated with control cells reduced this population (**Fig. 6F**). Taken together,
383 these results indicate that IFN-γ production by AML cells reshapes the BM microenvironment by
384 inducing Tregs through the upregulation of IDO1. The IFN-γ–dependent increase in Tregs is
385 positively associated with leukemia cell engraftment, suggesting the induction of an immune-
386 tolerant microenvironment.

Discussion

The ability of AML cells to shape the BM niche to their advantage is emerging as a hallmark of this cancer (2,3). Our study builds on this concept and demonstrates that the release of IFN-γ by AML cells skews the immunological composition of the BM microenvironment toward an immunosuppressive phenotype, enriched in suppressive Tregs, which correlates with worse clinical outcomes in AML patients.

AML cells produce a wide array of soluble mediators (40,41), which help them increase their autonomous growth capacity (42). Our study shows that AML cells have the ability to release IFN-γ. In contrast to other tumor models, where increased IFN-γ levels have been linked to cytokine production by infiltrating immune cells (43,44), our study found little, if any, contribution to IFN-γ secretion by the major immune cell subsets (i.e., $CD8^+$ and NK cells). Instead, we found that AML cells are the main source of IFN-γ. This finding reveals a unique feature of AML where IFN-γ production is more likely the result of an intrinsic dysregulation of leukemia cells rather than the consequence of inflammatory BM changes.

Moreover, our results unravel an unexpected tolerogenic role of IFN-γ in the context of AML, highlighting its 'dark side' in the creation of an immunosuppressive microenvironment. Indeed, in most tumors, IFN-γ is known to provide a signal resulting in enhanced anti-tumor immunity (20) and better clinical outcome (21-23). By contrast, in our AML patients' cohort, both microarray and NanoString analysis revealed an association of high *IFNG* expression with the upregulation of both inflammatory and, interestingly, immunosuppressive genes (e.g., IDO1 and NOS2). These data enabled us to identify a novel immune gene signature based on the 30 DEGs between $IFNG^{high}$ and $IFNG^{low}$ AML samples and create a prognostic index capable of dissecting AML patients into two groups with highly significant differences in survival. Notably, *IFNG* expression alone does not allow us to stratify AML patients from our cohort or public databases (our unpublished data), suggesting that the gene network of IFN-γ-related downstream signals is more relevant for patients'

outcomes. These results agree with previous observations that higher expression of type I and II IFN-related genes predicts chemotherapy resistance and response to immunotherapy in AML(45).

Increasing evidence indicates that Tregs are involved in creating an immune-tolerant BM microenvironment in AML. A high frequency of Tregs has been correlated with a reduced response to chemotherapy and poor overall survival (8-11). However, the mechanisms by which Tregs are induced within the BM are poorly understood. Moving from the observation that high IFN-γ production by AML cells positively correlates with increased Tregs in the BM of AML patients, we found that the silencing of IFN-γ expression in AML cells reduced the Treg frequency *in vivo*. This effect was paralleled by a decrease of IDO1 expression in BM cells, suggesting that the IDO1 pathway activation by IFN-γ–producing AML cells is crucial for Treg induction. IDO1 inhibition reduced the Treg subpopulation expressing CTLA-4, which regulates IDO1-mediated peripheral tolerance (46). Accordingly, an increase in a similar population of suppressive Tregs, expressing CTLA-4 and PD-1, was observed in IFN-γ^{high} BM samples. Together with the profound reshaping by AML cells of the BM cell transcriptome according to *IFNG* expression, these data suggest that Treg induction is part of a remodeling of the BM immune microenvironment initiated by AML cells through IFN-γ release. In this process, activation of the IDO1 pathway seemed central, corroborating previous reports that demonstrated a crucial role of IDO1 in orchestrating Treg induction in AML (47,48).

IFN-γ is the most potent inflammatory signal conferring immunosuppressive properties to MSCs (14,15). In particular, after exposure to IFN-γ, MSCs become able to induce fully functional Tregs *in vitro* and *in vivo* (12). We found that IFN-γ from AML cells altered gene expression in MSCs by up-regulating immune-tolerant and Treg differentiation pathways. Importantly, IFN-γ release by AML cells up-regulated MSC expression of IDO1 and its regulators. This observation was made both *in vitro* and *in vivo*. *In vitro*, IFN-γ release by AML cells primed MSCs to induce IDO1, which mediates Treg conversion. *In vivo*, silencing of IFN-γ expression in AML cells was associated with

a decrease of IDO1-expressing MSCs and Tregs. This result is in accordance with the finding of increased numbers of IDO1-expressing MSCs associated with high levels of Tregs in AML patients (49). It is conceivable that cells other than MSCs may participate in this process. In particular, AML cells have been described to increase IDO1 expression and activity after exposure to IFN-γ (47,48,50). Accordingly, *in vivo* ablation of IFN-γ production by AML cells reduced IDO1 expression, not only in MSCs. Thus, both AML cells and MSCs might contribute to establishing an immune-tolerant microenvironment via IDO1 However, in this work, we observed that, in a Treg conversion assay, AML cell contribution appears reduced if directly compared with that of the MSCs. Altogether, these data suggest that in the induction of Tregs via IDO1, the role of MSCs may be prominent, although the participation of other cell subsets cannot be ruled out.

In conclusion, this study shows that AML cells' ability to secrete IFN-γ enables them to alter the transcriptome of BM cells, leading to an immunosuppressive phenotype where induced Tregs have a prominent role. In such process, tolerogenic MSCs, as a key cellular component of BM niche and professional Treg-inducers, are likely to be pivotal. The newly emerging dual face of IFN-γ can be interpreted as part of the complex immune response in cancer, where the broad range of IFN-γ actions could depend on the context of tumor specificity, IFN-γ-signaling levels, and microenvironment conditions. A greater understanding of the IFN-γ–dependent tolerogenic tuning of the BM microenvironment could help provide a rationale for therapies able to overcome immune-modulatory effects on the stromal and immune microenvironment, such as IDO1 inhibitors, and may support the design of new treatments combining the activation of effector cell functions and inhibition of Tregs.

Authors' contributions

G. Corradi: Conceptualization, investigation, methodology. **B. Bassani**: investigation, methodology. **S. Sangaletti**: investigation, methodology, funding acquisition. **G. Simonetti**: investigation, methodology, formal analysis. **M. Fontana**: investigation, methodology. **M. Pazzaglia:** investigation, methodology. **A. Gulino**: investigation, methodology. **C. Tripodo:** investigation, methodology, formal analysis. **G. Cristiano:** Clinical data acquisition. **L. Bandini:** investigation, methodology. **E. Ottaviani:** investigation, methodology. **G. Martinelli:** Resources, funding acquisition. **M.P. Colombo**: funding acquisition, writing–review and editing. **J. Vadakekolathu**: investigation, methodology, formal analysis. **S. Rutella**: investigation, methodology, formal analysis, writing–original draft. **M. Cavo**: Resources, funding acquisition, writing–review and editing. **M. Ciciarello**: Conceptualization, funding acquisition, methodology, supervision, writing–original draft. **A. Curti**: Conceptualization, funding acquisition, supervision, writing–original draft. All authors read and approved the final manuscript.

Acknowledgements

We would like to thank Marie-Paule Vedrine and Bologna AIL (Associazione Italiana contro le Leucemie)/Section of Bologna for the kind support.

References

1. Yamashita M, Dellorusso PV, Olson OC, Passegué E. Dysregulated haematopoietic stem cell behaviour in myeloid leukaemogenesis. Nat Rev Cancer **2020**;20:365-82
2. Ciciarello M, Corradi G, Loscocco F, Visani G, Monaco F, Cavo M*, et al.* The Yin and Yang of the Bone Marrow Microenvironment: Pros and Cons of Mesenchymal Stromal Cells in Acute Myeloid Leukemia. Front Oncol **2019**;9:1135
3. Méndez-Ferrer S, Bonnet D, Steensma DP, Hasserjian RP, Ghobrial IM, Gribben JG*, et al.* Bone marrow niches in haematological malignancies. Nature Reviews Cancer **2020**;20:285-98
4. Brück O, Dufva O, Hohtari H, Blom S, Turkki R, Ilander M*, et al.* Immune profiles in acute myeloid leukemia bone marrow associate with patient age, T-cell receptor clonality, and survival. Blood Adv **2020**;4:274-86
5. Isidori A, Salvestrini V, Ciciarello M, Loscocco F, Visani G, Parisi S*, et al.* The role of the immunosuppressive microenvironment in acute myeloid leukemia development and treatment. Expert Rev Hematol **2014**;7:807-18
6. Buggins AG, Milojkovic D, Arno MJ, Lea NC, Mufti GJ, Thomas NS*, et al.* Microenvironment produced by acute myeloid leukemia cells prevents T cell activation and proliferation by inhibition of NF-kappaB, c-Myc, and pRb pathways. J Immunol **2001**;167:6021-30
7. Williams P, Basu S, Garcia-Manero G, Hourigan CS, Oetjen KA, Cortes JE*, et al.* The distribution of T-cell subsets and the expression of immune checkpoint receptors and ligands in patients with newly diagnosed and relapsed acute myeloid leukemia. Cancer **2019**;125:1470-81
8. Ustun C, Miller JS, Munn DH, Weisdorf DJ, Blazar BR. Regulatory T cells in acute myelogenous leukemia: is it time for immunomodulation? Blood **2011**;118:5084-95
9. Szczepanski MJ, Szajnik M, Czystowska M, Mandapathil M, Strauss L, Welsh A*, et al.* Increased frequency and suppression by regulatory T cells in patients with acute myelogenous leukemia. Clin Cancer Res **2009**;15:3325-32
10. Sallman DA, McLemore AF, Aldrich AL, Komrokji RS, McGraw KL, Dhawan A*, et al.* TP53 mutations in myelodysplastic syndromes and secondary AML confer an immunosuppressive phenotype. Blood **2020**;136:2812-23
11. Shenghui Z, Yixiang H, Jianbo W, Kang Y, Laixi B, Yan Z*, et al.* Elevated frequencies of $CD4^+$ $CD25^+$ CD127lo regulatory T cells is associated to poor prognosis in patients with acute myeloid leukemia. Int J Cancer **2011**;129:1373-81
12. Yan Z, Zhuansun Y, Chen R, Li J, Ran P. Immunomodulation of mesenchymal stromal cells on regulatory T cells and its possible mechanism. Exp Cell Res **2014**;324:65-74
13. Morrison SJ, Scadden DT. The bone marrow niche for haematopoietic stem cells. Nature **2014**;505:327-34
14. Krampera M, Cosmi L, Angeli R, Pasini A, Liotta F, Andreini A*, et al.* Role for interferon-gamma in the immunomodulatory activity of human bone marrow mesenchymal stem cells. Stem Cells **2006**;24:386-98
15. Meisel R, Zibert A, Laryea M, Gobel U, Daubener W, Dilloo D. Human bone marrow stromal cells inhibit allogeneic T-cell responses by indoleamine 2,3-dioxygenase-mediated tryptophan degradation. Blood **2004**;103:4619-21
16. Platten M, Friedrich M, Wainwright DA, Panitz V, Opitz CA. Tryptophan metabolism in brain tumors - IDO and beyond. Curr Opin Immunol **2021**;70:57-66
17. Hanahan D, Weinberg RA. Hallmarks of cancer: the next generation. Cell **2011**;144:646-74

18. Grivennikov SI, Greten FR, Karin M. Immunity, inflammation, and cancer. Cell **2010**;140:883-99
19. de Bruin AM, Voermans C, Nolte MA. Impact of interferon-γ on hematopoiesis. Blood **2014**;124:2479-86
20. Ivashkiv LB. IFNγ: signalling, epigenetics and roles in immunity, metabolism, disease and cancer immunotherapy. Nat Rev Immunol **2018**;18:545-58
21. Overacre-Delgoffe AE, Chikina M, Dadey RE, Yano H, Brunazzi EA, Shayan G, *et al.* Interferon-γ Drives T. Cell **2017**;169:1130-41.e11
22. Fridman WH, Pagès F, Sautès-Fridman C, Galon J. The immune contexture in human tumours: impact on clinical outcome. Nature Reviews Cancer **2012**;12:298-306
23. Sangro B, Sarobe P, Hervás-Stubbs S, Melero I. Advances in immunotherapy for hepatocellular carcinoma. Nat Rev Gastroenterol Hepatol **2021**;18:525-43
24. Zaidi MR, Merlino G. The two faces of interferon-γ in cancer. Clin Cancer Res **2011**;17:6118-24
25. Simonetti G, Angeli D, Petracci E, Fonzi E, Vedovato S, Sperotto A, *et al.* Adrenomedullin Expression Characterizes Leukemia Stem Cells and Associates With an Inflammatory Signature in Acute Myeloid Leukemia. Front Oncol **2021**;11:684396
26. Simonetti G, Padella A, do Valle IF, Fontana MC, Fonzi E, Bruno S, *et al.* Aneuploid acute myeloid leukemia exhibits a signature of genomic alterations in the cell cycle and protein degradation machinery. Cancer **2019**;125:712-25
27. Metsalu T, Vilo J. ClustVis: a web tool for visualizing clustering of multivariate data using Principal Component Analysis and heatmap. Nucleic Acids Res **2015**;43:W566-70
28. Kuleshov MV, Jones MR, Rouillard AD, Fernandez NF, Duan Q, Wang Z, *et al.* Enrichr: a comprehensive gene set enrichment analysis web server 2016 update. Nucleic Acids Res **2016**;44:W90-7
29. Wagner S, Vadakekolathu J, Tasian SK, Altmann H, Bornhäuser M, Pockley AG, *et al.* A parsimonious 3-gene signature predicts clinical outcomes in an acute myeloid leukemia multicohort study. Blood Adv **2019**;3:1330-46
30. Ley TJ, Miller C, Ding L, Raphael BJ, Mungall AJ, Robertson A, *et al.* Genomic and epigenomic landscapes of adult de novo acute myeloid leukemia. N Engl J Med **2013**;368:2059-74
31. Liu W, Putnam AL, Xu-Yu Z, Szot GL, Lee MR, Zhu S, *et al.* CD127 expression inversely correlates with FoxP3 and suppressive function of human CD4+ T reg cells. J Exp Med **2006**;203:1701-11
32. Miyara M, Yoshioka Y, Kitoh A, Shima T, Wing K, Niwa A, *et al.* Functional delineation and differentiation dynamics of human CD4+ T cells expressing the FoxP3 transcription factor. Immunity **2009**;30:899-911
33. Wang X, Lang M, Zhao T, Feng X, Zheng C, Huang C, *et al.* Cancer-FOXP3 directly activated CCL5 to recruit FOXP3. Oncogene **2017**;36:3048-58
34. Lv M, Xu Y, Tang R, Ren J, Shen S, Chen Y, *et al.* miR141-CXCL1-CXCR2 signaling-induced Treg recruitment regulates metastases and survival of non-small cell lung cancer. Mol Cancer Ther **2014**;13:3152-62
35. Puccetti P, Grohmann U. IDO and regulatory T cells: a role for reverse signalling and non-canonical NF-kappaB activation. Nat Rev Immunol **2007**;7:817-23
36. Tas SW, Vervoordeldonk MJ, Hajji N, Schuitemaker JH, van der Sluijs KF, May MJ, *et al.* Noncanonical NF-kappaB signaling in dendritic cells is required for indoleamine 2,3-dioxygenase (IDO) induction and immune regulation. Blood **2007**;110:1540-9
37. Tripodo C, Burocchi A, Piccaluga PP, Chiodoni C, Portararo P, Cappetti B, *et al.* Persistent Immune Stimulation Exacerbates Genetically Driven Myeloproliferative Disorders via Stromal Remodeling. Cancer Res **2017**;77:3685-99

38. Sato K, Ozaki K, Oh I, Meguro A, Hatanaka K, Nagai T, *et al.* Nitric oxide plays a critical role in suppression of T-cell proliferation by mesenchymal stem cells. Blood **2007**;109:228-34
39. Wing K, Onishi Y, Prieto-Martin P, Yamaguchi T, Miyara M, Fehervari Z, *et al.* CTLA-4 control over Foxp3+ regulatory T cell function. Science **2008**;322:271-5
40. Tobler A, Moser B, Dewald B, Geiser T, Studer H, Baggiolini M, *et al.* Constitutive expression of interleukin-8 and its receptor in human myeloid and lymphoid leukemia. Blood **1993**;82:2517-25
41. Bradbury D, Rogers S, Reilly IA, Kozlowski R, Russell NH. Role of autocrine and paracrine production of granulocyte-macrophage colony-stimulating factor and interleukin-1 beta in the autonomous growth of acute myeloblastic leukaemia cells--studies using purified CD34-positive cells. Leukemia **1992**;6:562-6
42. Lotem J, Sachs L. Cytokine control of developmental programs in normal hematopoiesis and leukemia. Oncogene **2002**;21:3284-94
43. Takeda K, Nakayama M, Hayakawa Y, Kojima Y, Ikeda H, Imai N, *et al.* IFN-γ is required for cytotoxic T cell-dependent cancer genome immunoediting. Nat Commun **2017**;8:14607
44. Abiko K, Matsumura N, Hamanishi J, Horikawa N, Murakami R, Yamaguchi K, *et al.* IFN-γ from lymphocytes induces PD-L1 expression and promotes progression of ovarian cancer. Br J Cancer **2015**;112:1501-9
45. Vadakekolathu J, Minden MD, Hood T, Church SE, Reeder S, Altmann H, *et al.* Immune landscapes predict chemotherapy resistance and immunotherapy response in acute myeloid leukemia. Sci Transl Med **2020**;12
46. Mellor AL, Baban B, Chandler P, Marshall B, Jhaver K, Hansen A, *et al.* Cutting edge: induced indoleamine 2,3 dioxygenase expression in dendritic cell subsets suppresses T cell clonal expansion. J Immunol **2003**;171:1652-5
47. Curti A, Pandolfi S, Valzasina B, Aluigi M, Isidori A, Ferri E, *et al.* Modulation of tryptophan catabolism by human leukemic cells results in the conversion of CD25- into CD25+ T regulatory cells. Blood **2007**;109:2871-7
48. Curti A, Trabanelli S, Salvestrini V, Baccarani M, Lemoli RM. The role of indoleamine 2,3-dioxygenase in the induction of immune tolerance: focus on hematology. Blood **2009**;113:2394-401
49. Mansour I, Zayed RA, Said F, Latif LA. Indoleamine 2,3-dioxygenase and regulatory T cells in acute myeloid leukemia. Hematology **2016**;21:447-53
50. Curti A, Aluigi M, Pandolfi S, Ferri E, Isidori A, Salvestrini V, *et al.* Acute myeloid leukemia cells constitutively express the immunoregulatory enzyme indoleamine 2,3-dioxygenase. Leukemia. England2007. p 353-5.

618 **Figure 1**

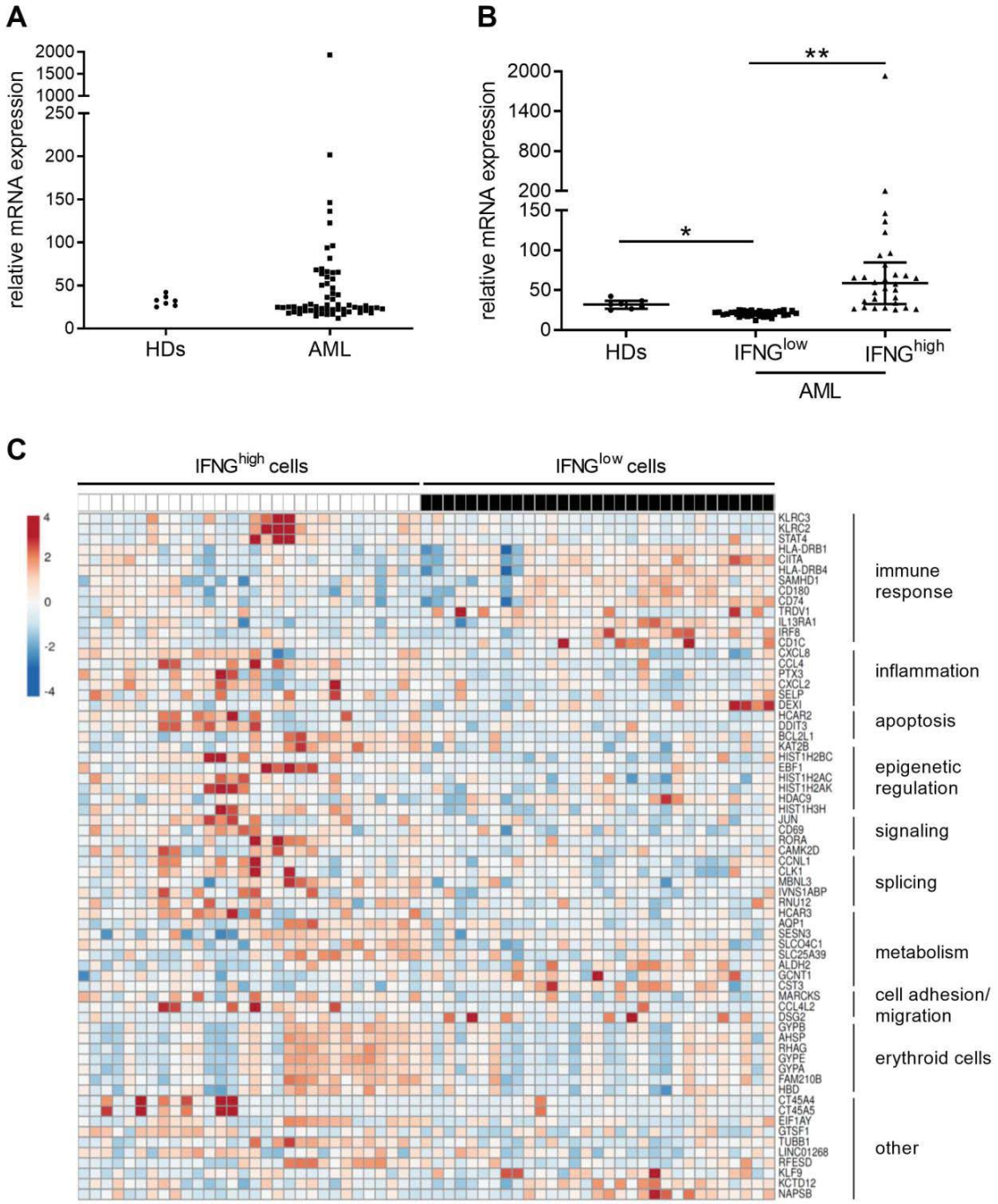

619

620 **Figure 1.** *IFNG* expression in AML samples is highly variable. **A,** Relative expression of *IFNG*

621 mRNA in BM-derived mononuclear cells from 7 healthy donors (HDs) and 61 AML patients at

622 diagnosis. **B,** Relative expression of *IFNG* mRNA in HDs and AML samples dichotomized into

IFNG^{low} (n=31) and IFNG^{high} (n=30) groups at the median. Horizontal lines indicate the median and interquartile range (HDs vs IFNG^{low},* P=0.008; HDs vs IFNG^{high}, P= 0.551; IFNG^{low} vs IFNG^{high}, **P<0.001; Kruskal-Wallis-test). **C,** Heatmap of differentially expressed genes (|FC|≥2.0 and P≤0.05) between IFNG^{high} and IFNG^{low} AML cells. Columns represent patients. Color changes within rows indicate expression levels relative to the mean for each gene, rescaled on the standard deviation. Genes are ranked according their fold chance (from high to low, IFNG^{high}/ IFNG^{low}) inside each macro-pathway (shown on the right).

649

Figure 2

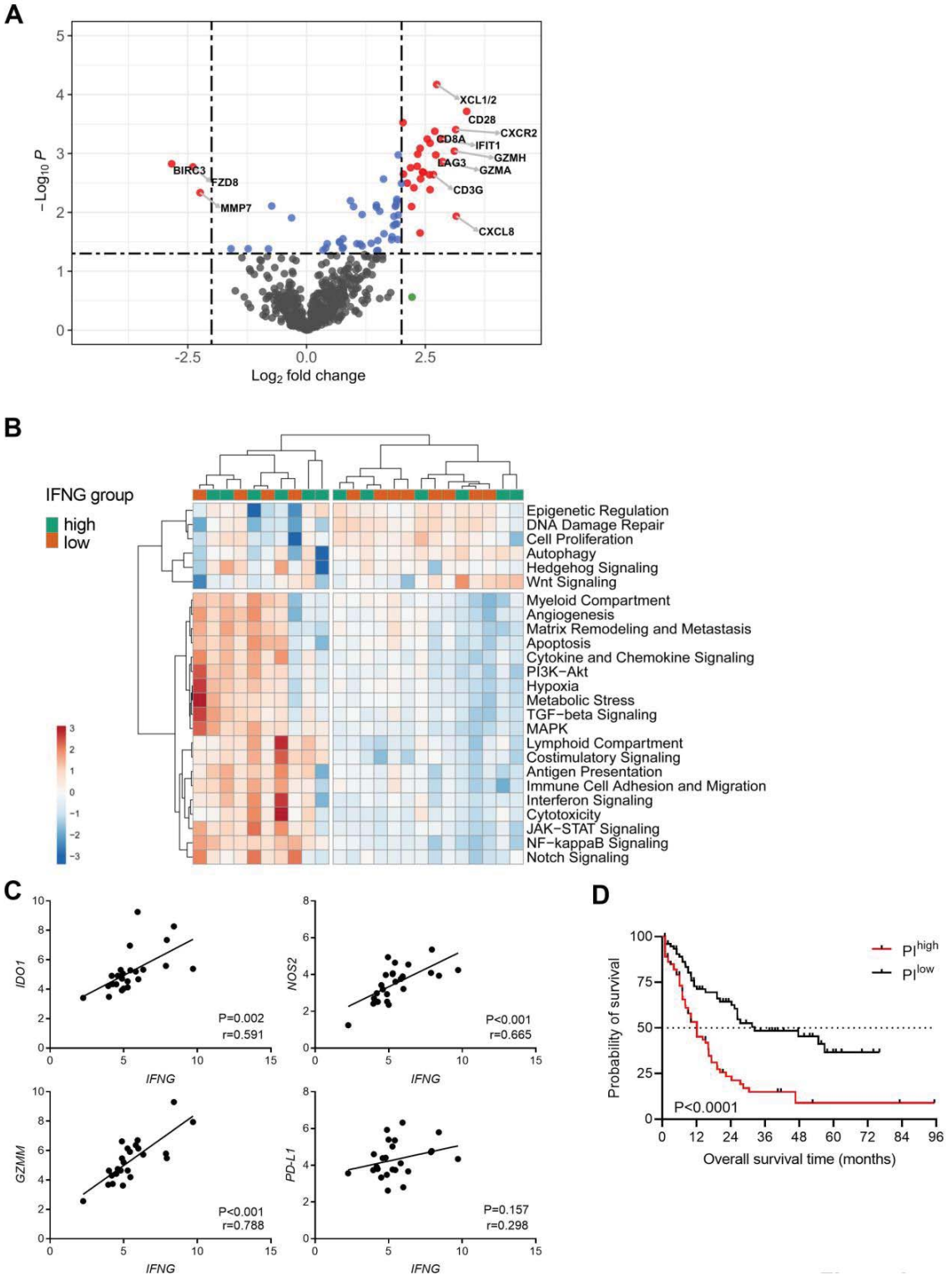

650

Figure 2. IFNG^{high} AML cells express a distinctive inflammatory and immune gene signature correlated to poor overall survival. **A,** Volcano plot showing differentially expressed genes between IFNG^{low} and IFNG^{high} groups. Log2 fold change (FC) threshold, 2; *P* value threshold, 0.01 (false discovery rate). Red dots: |log2 FC|>2 and $P<0.05$. **B,** Heatmap of nSolver biological activity and pathway scores calculated as linear combinations of pre-defined gene sets. Samples and genes are sorted by unsupervised hierarchical clustering, using Euclidean distance and complete linkage. **C,** Pearson's correlations between NanoString-derived mRNA levels of *IFNG* and *IFNG*-modulated immune-related genes. **D,** Kaplan-Meier analysis of overall survival for 149 AML patients dichotomized according to prognostic index in PI^{high} group (n=74) and PI^{low} group (n=75). Log-rank test.

672

Figure 3

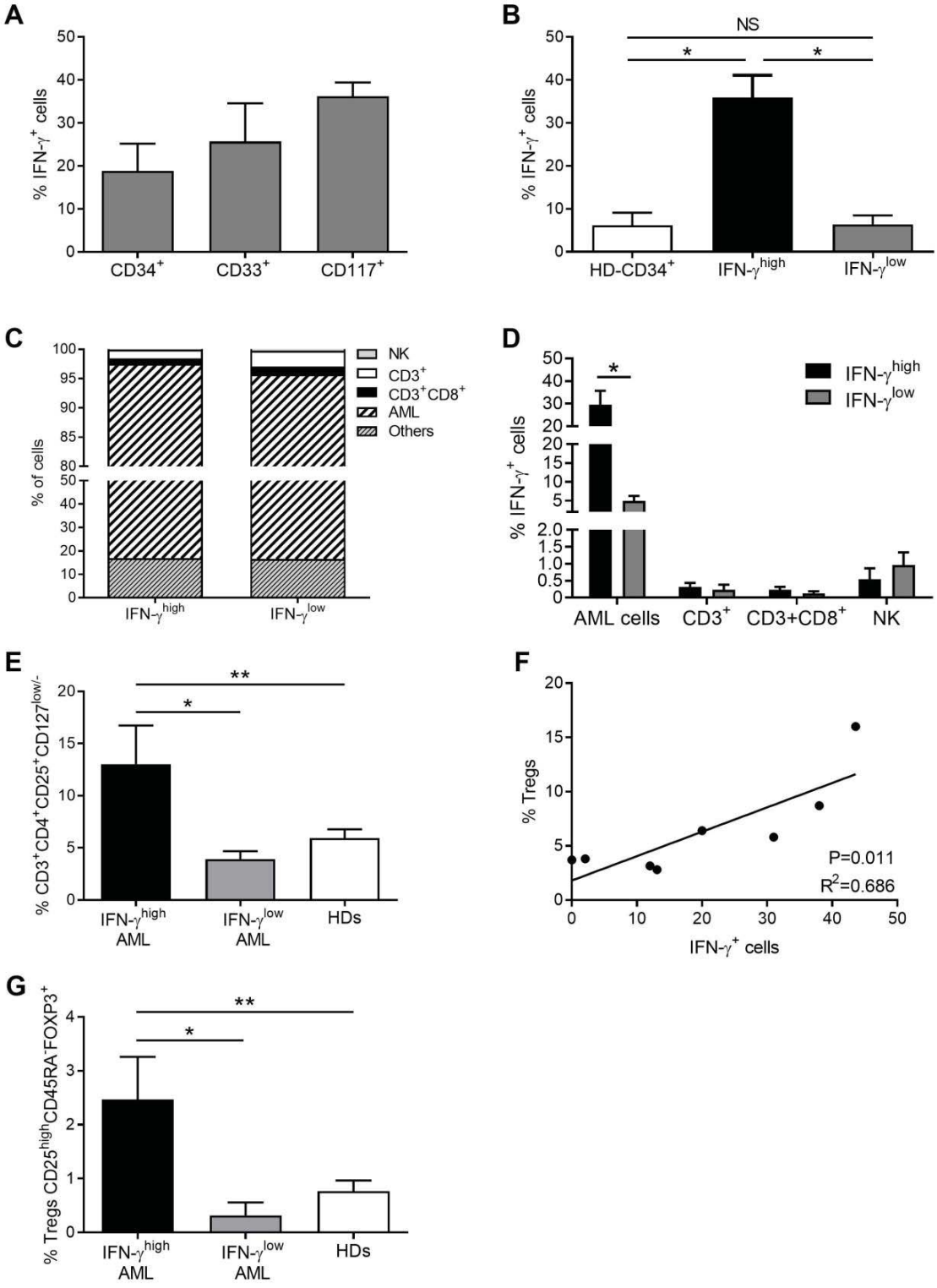

673

Figure 3. IFN-γ expressed by BM AML cells correlates with the presence of Tregs in the BM. **A,** Cells co-expressing IFN-γ and the indicated blast-specific marker analyzed by flow cytometry (mean ± SEM, n=12; CD34 vs CD33, *P*=0.875; CD34 vs CD117, *P*=0.623; CD33 vs CD117, *P*=0.792; one-way ANOVA, Tukey comparison). **B,** IFN-γ^+ cells in immune-magnetically purified $CD34^+$ cells from healthy BM donors (n=4) and in IFN-γ^{high} (n=8) and IFN-γ^{low} samples (n=8) (mean ± SEM; **P*<0.001, NS, not significant; one-way ANOVA, Bonferroni correction for multiple comparisons). **C,** Cellular composition of IFN-γ^{high} and IFN-γ^{low} samples by flow cytometry. AML cells ($CD34^+$, $CD33^+$, or $CD117^+$); NK cells ($CD45^+CD3^-CD56^+$). Values are averages of at least 5 samples (*P*>0.05, two-way ANOVA, Bonferroni correction for multiple comparisons). **D,** IFN-γ^+ cells in IFN-γ^{high} (n=7) and IFN-γ^{low} (n=7) groups, by cell type (mean ± SEM; **P*<0.001; two-way ANOVA, Bonferroni correction for multiple comparisons. **E,** Frequencies of Tregs ($CD3^+CD4^+CD25^+CD127^{low/-}$ cells) in BM cells of healthy donors (HDs; n=5) and in IFN-γ^{high} (n=4) and IFN-γ^{low} (n=7) samples (mean ± SEM; **P*=0.005, ***P*=0.040; one-way ANOVA, Tukey comparison). **F,** Correlation between the percentages of Tregs and IFN-γ^+ cells in BM cells (linear regression). **G,** Activated, suppressive Tregs ($CD45RA^-CD25^{high}FOXP3^+$ cells) within the $CD3^+CD4^+CD25^+CD127^{low/-}$ Treg population, expressed as a percentage of $CD4^+$ cells, in BM cells of healthy donors (n=5) and in IFN-γ^{high} (n=4) and IFN-γ^{low} (n=7) samples (mean ± SEM; **P*=0.008, ***P*=0.041; one-way ANOVA, Tukey comparison).

697

Figure 4

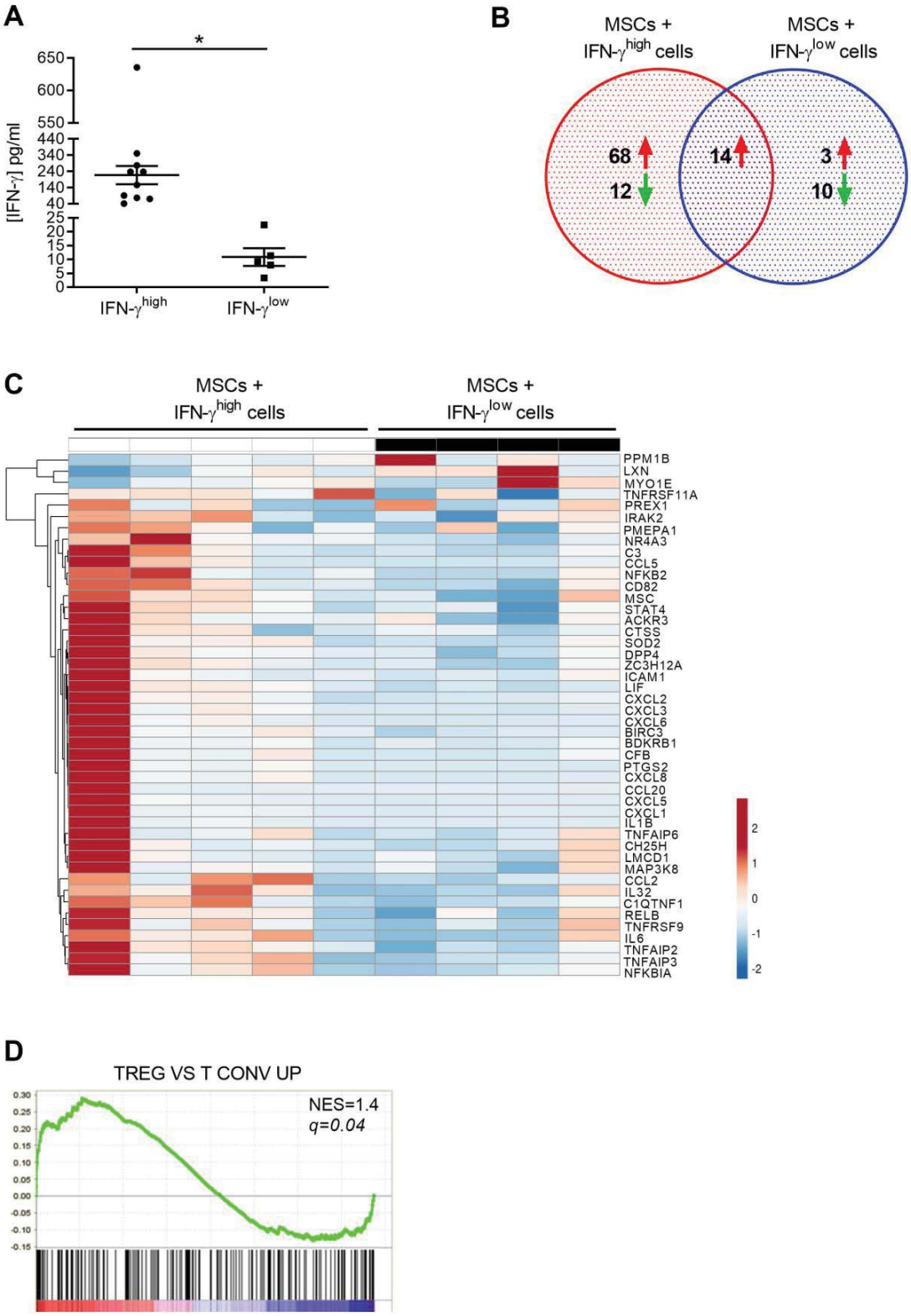

698

Figure 4. IFN-γ^{high} AML cells mold the MSC transcriptome towards an immunosuppressive profile. **A,** IFN-γ levels in conditioned medium from co-cultures of MSCs and IFN-γ^{high} or IFN-γ^{low} cells. Each dot represents the average of one sample analyzed by immunoassay in triplicate (mean ± SEM of at least 5 experiments with different samples; **P*=0.025; unpaired *t* test. **B,** Venn diagram showing numbers of genes up-regulated and down-regulated in MSCs co-cultured with IFN-γ^{high} (n=5) or IFN-γ^{low} (n=4) cells with respect to MSC monocultures (n=5). **C,** Heatmap of selected immune response-related genes whose expression in MSCs changed as a result of co-culture with IFN-γ^{high} or IFN-γ^{low} cells. Columns report ratios between a co-culture and its related monoculture. Color scale indicates expression levels relative to the mean for each gene, rescaled on the standard deviation. Genes are sorted by average linkage hierarchical clustering. **D,** Representative enplot from gene set enrichment analysis of immune tolerance signatures in MSCs co-cultured with IFN-γ^{high} cells. The illustrated pathway (TREG VS T CONV UP) refers to the up-regulation of Treg differentiation from conventional T cells. NES, normalized enrichment score; *q*, FDR *q* value.

Figure 5

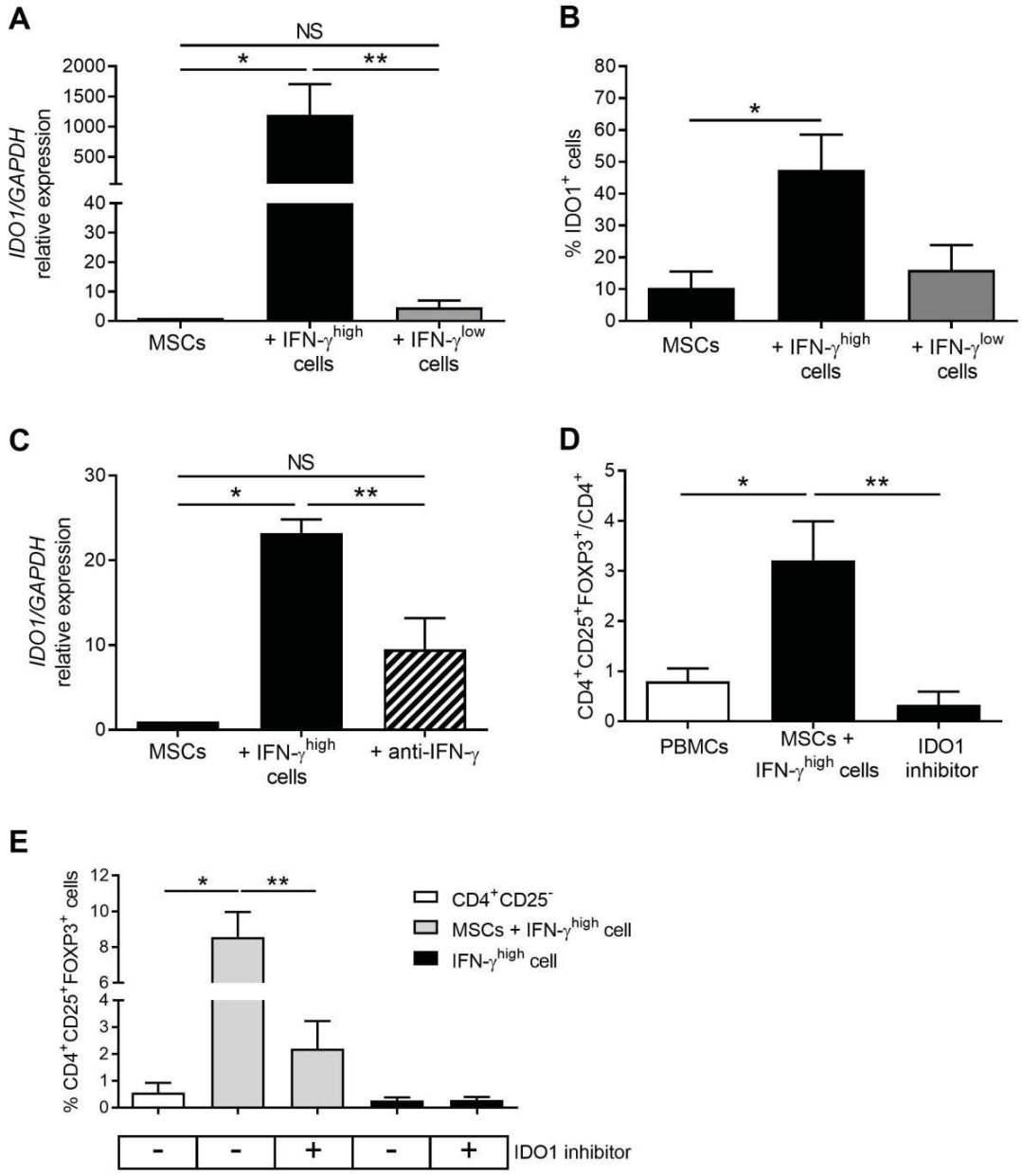

Figure 5. IFN-γ^{high} cells induce IDO1 expression in MSCs and increase their capacity to induce Tregs. **A,** qRT-PCR analysis of *IDO1* gene expression in MSCs cultured for 4 days, alone (taken as 1) or with IFN-γ^{high} or IFN-γ^{low} cells (mean ± SEM of 5 experiments; **P*=0.004, ***P*=0.005; one-way ANOVA, Bonferroni correction for multiple comparisons). **B,** Percentage of IDO1^{+} cells analyzed by flow cytometry in MSCs cultured for 4 days, alone or with IFN-γ^{high} or IFN-γ^{low} cells

(mean ± SEM of 3 experiments; MSCs vs IFN-γ^{high}, *P=0.039; MSCs vs IFN-γ^{low}, P=0.581; IFN-γ^{high} vs IFN-γ^{low}, P=0.082; one-way ANOVA, Bonferroni correction for multiple comparisons). **C,** qRT-PCR analysis of *IDO1* expression in MSCs cultured for 6 h, alone or with IFN-γ^{high} cells, in the absence or presence of an IFN-γ-neutralizing antibody (anti-IFN-γ, 20 μg/ml) (mean ± SEM of 3 experiments; *P<0.001, **P=0.012; one-way ANOVA, Tukey correction). **D,** Percentages of Tregs ($CD3^+CD4^+CD25^+FOXP3^+$ T cells, gated on $CD4^+$) in 7-day cultures of PBMCs alone or with MSCs pre-cultured with IFN-γ^{high} cells for 4 days, in the absence or presence of 1 mM 1-methyl-DL-tryptophan (mean ± SEM of 6 experiments; *P=0.004; **P=0.002; one-way ANOVA, Tukey correction). **E,** Percentage of $CD4^+CD25^+FOXP3^+$ cells after 7-day cultures of purified $CD4^+CD25^-$ T cells, alone or with MSCs pre-cultured for 4 days with IFN-γ^{high} cells, in the absence or presence of 1 mM 1-methyl-DL-tryptophan (mean ± SEM of 5 experiments; *P<0.001, **P=0.001; one-way ANOVA, Tukey correction).

753 **Figure 6**

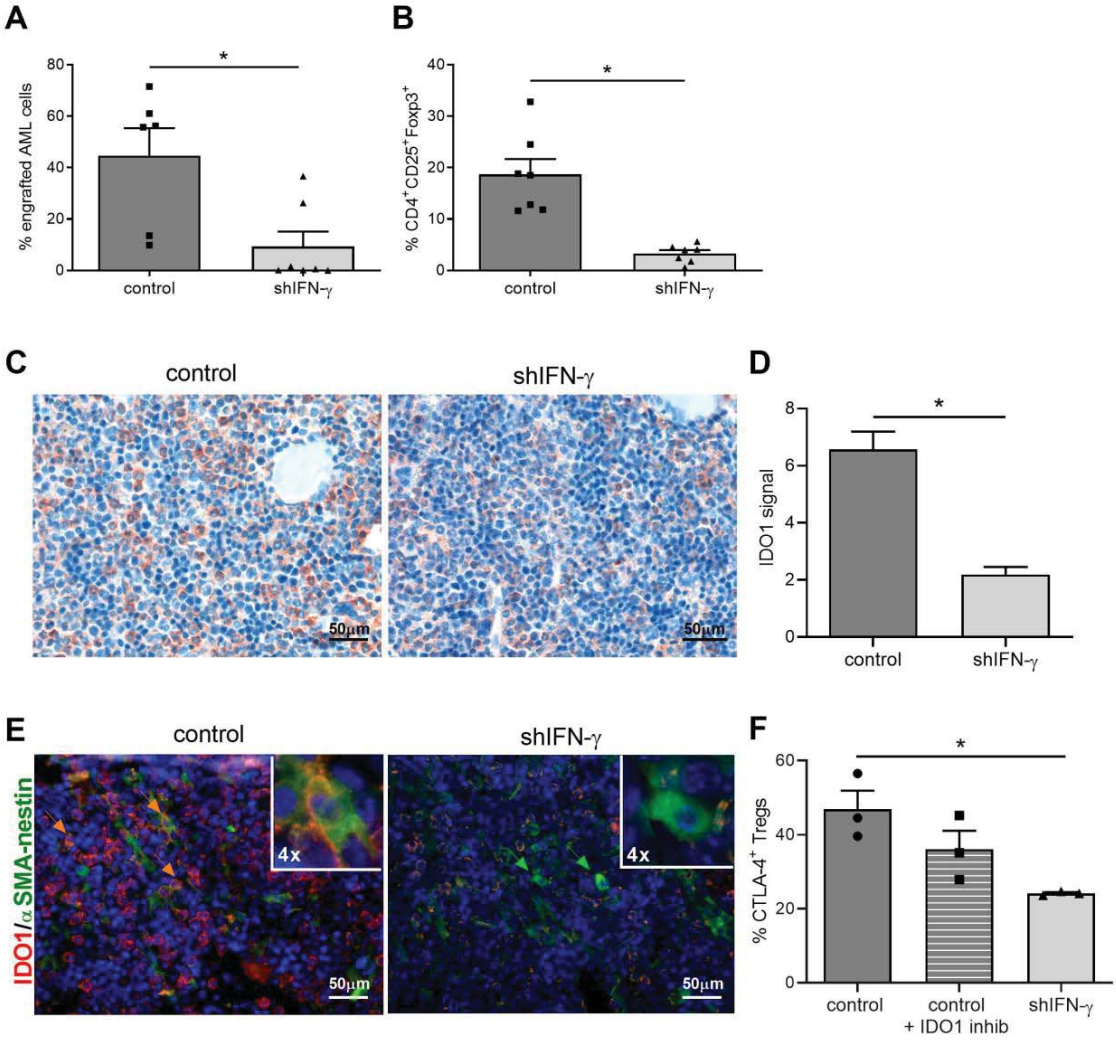

754

755 **Figure 6.** IFN-γ production by AML cells shapes the BM microenvironment by inducing Tregs *in*
756 *vivo*. Tibia of C57BL/6 mice were injected with C1498 cells transfected with a vector expressing
757 *Ifng*-specific or non-specific shRNA (shIFN-γ or control). After 31 days, BM was flushed to obtain
758 cells for flow cytometry and bone was paraffin-embedded for microscopy. **A,** Engraftment (31
759 days) of BM cells expressing GFP (control, n=6; shIFN-γ, n=7; **P*=0.011; unpaired *t* test). **B,**
760 Frequencies of Tregs ($CD4^+CD25^+Foxp3^+$cells) gated on $CD4^+$ cells (control, n=7; shIFN-γ, n=7;
761 **P*<0.001; unpaired *t* test). **C,** Immunohistochemistry of IDO1 in BM sections. Magnification ×40.
762 **D,** Quantification of IDO1 staining of sections in C. Values are percentages of positive signals (3+

and 2+) in five non-overlapping high-power fields (×400) per group; *P<0.001, unpaired t test. **E,** Immunofluorescence in BM sections of IDO1 (red, Alexa Fluor 568), αSMA–nestin (green, Alexa Fluor 488), and triple-positive cells (yellow). Blue, nuclei (DAPI). Magnification 40×. Representative arrowed cells are shown magnified in the inserts. **F,** CTLA-4$^+$ Tregs expressed as a percentage of all Tregs (control, n=3; control +IDO1 inhib, n=3; shIFN-γ, n=3; control vs control +IDO1 inhib, P=0.229; control +IDO1 inhib vs shIFN-γ, P=0.180; control vs shIFN-γ, *P=0.018; one-way ANOVA, Tukey comparison). Values are mean and SEM in all experiments.